

Haptic Palpation for Medical Simulation in Virtual Environments

Sebastian Ullrich, *Student Member, IEEE*, and Torsten Kuhlen

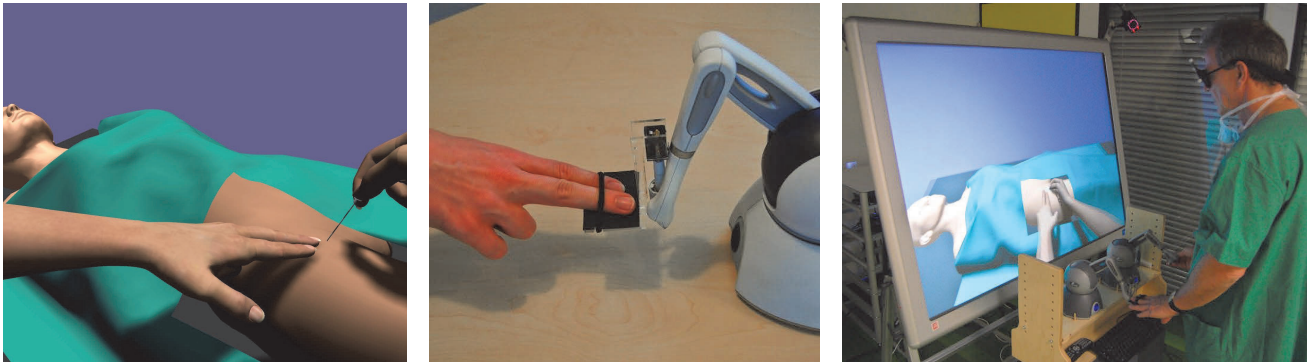


Fig. 1. A closeup of palpation interaction on a virtual patient (left), a lightweight palpation pad as a hardware modification for a haptic device (middle), and a medical training simulator prototype used by a medical expert (right).

Abstract—Palpation is a physical examination technique where objects, e.g., organs or body parts, are touched with fingers to determine their size, shape, consistency and location. Many medical procedures utilize palpation as a supplementary interaction technique and it can be therefore considered as an essential basic method. However, palpation is mostly neglected in medical training simulators, with the exception of very specialized simulators that solely focus on palpation, e.g., for manual cancer detection. In this article we propose a novel approach to enable haptic palpation interaction for virtual reality-based medical simulators. The main contribution is an extensive user study conducted with a large group of medical experts. To provide a plausible simulation framework for this user study, we contribute a novel and detailed interaction algorithm for palpation with tissue dragging, which utilizes a multi-object force algorithm to support multiple layers of anatomy and a pulse force algorithm for simulation of an arterial pulse. Furthermore, we propose a modification for an off-the-shelf haptic device by adding a lightweight palpation pad to support a more realistic finger grip configuration for palpation tasks. The user study itself has been conducted on a medical training simulator prototype with a specific procedure from regional anesthesia, which strongly depends on palpation. The prototype utilizes a co-rotational finite-element approach for soft tissue simulation and provides bimanual interaction by combining the aforementioned techniques with needle insertion for the other hand. The results of the user study suggest reasonable face validity of the simulator prototype and in particular validate medical plausibility of the proposed palpation interaction algorithm.

Index Terms—Medicine, physically-based simulation, haptics, user studies.

1 INTRODUCTION

There are numerous reasons for medical simulation, e.g., ethical issues, patient safety, training, pre-operation planning and warm up. Benefits of virtual reality-based (VR) medical simulation are, exchangeable scenarios, fully controllable environments, automated assessment, unlimited repetitions, etc., and have been proven in various studies. Many medical procedures are often preceded or accompanied by palpation. Palpation can be defined as a manual technique and is usually used for localization and confirmation of anatomical landmarks such as bones, muscles and pulse. It requires anatomical knowledge, practical experience and the sense of touch to identify these subcutaneous anatomical landmarks. Therefore, its inclusion in training simulators could be beneficial.

The article is structured as follows. First, we provide an overview of related work in Section 2. In Section 3 follows one contribution of the article with a novel palpation interaction approach, which combines tissue dragging and rendering of various haptic effects. Section

4 explains how to construct a palpation pad as a hardware extension for a haptic device. Finally, the main contribution of this article is in Section 5 and consists of an extensive user study with medical experts. It evaluates a simulation prototype with a specific medical procedure that utilizes the aforementioned solutions for palpation interaction.

2 RELATED WORK

A survey on simulators for palpation training [44] discriminates between three categories: physical, virtual and hybrid. In the following, we will focus on VR-based approaches and a few hybrid approaches.

In the nineties, several palpation simulators were based on the Rutgers Master II force feedback glove [17]. The first simulator application with this device was developed for training of knee palpation [27]. Another simulator, also with this force feedback glove, was created for abdominal palpation to detect subsurface liver tumor [14]. It featured multiple finger support and used deformation depth for lookup in force deflection curves. These force deflection curves were acquired in a controlled environment, either from measuring on gel phantoms, or from calculating off-line finite element method (FEM) simulations. Bureda et al. [6] developed a simulation to train the detection of prostate cancer. A PHANTOM haptic device was used with a thimble attached to the end-effector. The force calculation was based on a modified non-linear Hooke's law equation with subjectively chosen stiffness parameters. Another simulator for prostate examination [24] utilizes FEM to simulate collision of two meshes with very low resolution (200 nodes in total) representing internal organs for indirect

- Sebastian Ullrich is with Virtual Reality Group, RWTH Aachen University and SenseGraphics AB, E-mail: s.ullrich@ieee.org.
- Torsten Kuhlen is with Virtual Reality Group, RWTH Aachen University, E-mail: kuhlen@vr.rwth-aachen.de.

Manuscript received 15 September 2011; accepted 3 January 2012; posted online 4 March 2012; mailed on 27 February 2012.

For information on obtaining reprints of this article, please send email to: tvcg@computer.org.

palpation. The work of Crossan et al. [12] focused on simulation for horse ovary palpation in veterinary training with a PHANTOM haptic device. The same group later on created two hybrid simulators: one for bovine rectal palpation [5] with the PHANTOM haptic device inside a fiberglass model of a cow's back [4] and another one for feline abdominal palpation [33] with two PHANTOM devices and a cat puppet. At Ohio University the Virtual Haptic Back was developed [43]. In this simulator the bone segments of the spine can be explored and manipulated by the index fingers through thimbles attached to two PHANTOM devices. The simulation is based on a combination of rigid body dynamics and a simple mass-spring system. A further approach for haptic rendering of palpation has been proposed in [8]. The simulator utilizes a PHANTOM desktop device and proposes a contact model for the fingertips based on Hertz's deformation theory [26]. One of the first simulators for breast palpation utilizes a PHANTOM device and a static breast model [1]. A hybrid approach [16] combined a silicon breast with a dynamic pulse simulation and compared it to a static silicon model. The Haptic Interface Robot (HIRO) device consists of a force actuated 6DOF arm and 3 fingers with 3DOF force output [22]. This system was used in a simulator for breast palpation [2]. In this simulator the breast tissue is simulated with a simplified FEM mesh utilizing the condensation technique to only compute deformations of the surface nodes [13]. Recently, the simulator has been updated with the five-fingered HIRO III device [15]. In a mixed-reality approach, pulse simulation has been achieved with pneumatic augmentation of cadavers [37]. Whilst effective, the approach is costly and ethically questionable. Another system [25] combines a PHANTOM haptic device with a pin-array tactile display for area-based haptic rendering and compares it with point-based haptic rendering in a user study. A simulator for the femoral pulse [9] compares three different tactile actuators: piezoelectric pads, micro speakers and a pin-array display. In a follow-up work from the same authors [10] the femoral pulse is simulated with a hydraulics-based pad mounted on one modified NovInt Falcon haptic device.

In summary, there are already many interesting approaches for palpation simulation. However, most of these solutions are very much optimized for a specific procedure and thus difficult to apply to other procedures. Furthermore, most solutions focus on a detailed description of the haptic rendering and only briefly mention deformation without providing algorithmic details. If deformations are supported, then mass-spring systems are often utilized instead of the more versatile and continuum mechanics-based FEM. User studies are lacking completely in most of the approaches. In contrast, our approach has been successfully tested with a FEM-based soft tissue simulation, provides a detailed description of the algorithms for tissue dragging and haptic rendering, proposes a hardware modification and employs a user study to assess face validity of the simulator.

3 PALPATION INTERACTION

Palpation is a physical examination technique where fingers are utilized in prehensile motions, e.g., grasping and seizing, and non-prehensile motions, e.g., pushing and lifting [31]. In the following, we focus on non-prehensile movements. Consequently, the soft tissue, represented in our simulation by tetrahedral *behavior meshes*, should be deformable and draggable during sliding motions depending on surface friction. In the following, we first propose a visual coupling to prevent object intersections in the visual feedback, describe a tissue dragging approach and then specify two force rendering algorithms that are essential for palpation simulation.

3.1 Visual Coupling

For visual feedback during palpation interaction, we use a *visual coupling*-approach between the device tool center point T_{CP} and the visual model center point V_{CP} , where V_{CP} transforms the virtual hand's geometry (see Figure 2). One option would be to optimize the discrepancy by position and velocity [7]. Our approach is loosely related to virtual coupling [11] and the god-object proxy [45] and works as follows. In its neutral state, the T_{CP} resides at the finger tip that is used as "palpation-sensor". Furthermore, for collision detection a ray

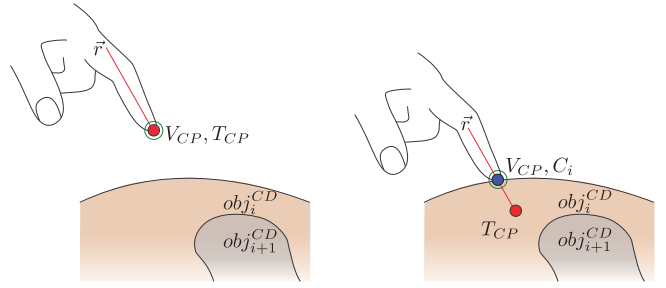


Fig. 2. Schematic overview of visual coupling between the visual model center point V_{CP} and input device tool center point T_{CP} . Without collisions V_{CP} equals T_{CP} (left). However, when the device ray \vec{r} collides with the skin surface $ob_j_i^{CD}$, V_{CP} is constrained to the current contact point C_i (right).

\vec{r} is attached to T_{CP} and aligned to the palpating finger (see Figure 2, left). Collisions are checked with a triangle-ray test, implemented in the Bullet Physics Library, using the ray \vec{r} and testing against objects $ob_j_i^{CD}$ of the virtual patient. Those objects represent all palpable structures in the virtual patient, e.g., skin surface, hip bone, and muscle lodges. If there are no collisions, the visual model is transformed by the device tool center point: $V_{CP} = T_{CP}$ (see Figure 2, left). However, if there is a collision between the ray \vec{r} and an object $ob_j_i^{CD}$, the intersection point is stored as C_i . In this case, T_{CP} can intersect and penetrate the skin surface and other structures, while the visual model of the virtual hand is constrained to the current contact point C_i on the skin surface: $V_{CP} = C_i$ (see Figure 2, right).

3.2 Tissue Dragging

We propose a novel algorithm (see pseudo code in Figure 3) with tissue dragging to simulate palpation interaction between a virtual hand controlled by the user and the soft tissue of a virtual patient as follows. Dragging only occurs during contact with the skin surface. First, the nearest surface node B_i of the behavior mesh relative to the collision point C_i is searched by proximity search. For dragging in normal direction, we use a Hookean spring constraint cs_i between B_i and the device position T_{CP} projected to the contact normal \vec{n}_i with a stiffness value k depending on the tissue type (see Figure 4):

$$\vec{f}_{B_i}^n = -((B_i - T_{CP}) \cdot \vec{n}_i) \vec{n}_i k. \quad (1)$$

To determine the lateral dragging behavior for the skin surface, any appropriate friction model with stick-slip behavior can be applied, e.g., Karnopp friction [21] or one of the friction models summarized in a survey [3]. In a first approach, we assume that friction of the finger in the stick phase is proportional to the normal force [30]. Depending on the magnitude of the finger's pressure, i.e., force in normal direction \vec{f}_{n_i} , we switch between stick and slip states, where f_{stick} is a threshold based on real-world measurements [20, 36]. During the stick state, we save the initial contact point C_i' and compute the lateral stretching distance d_{lat} based on the visual model's center point of the tool V_{CP} , i.e., the virtual finger position (collision point) on the skin surface:

$$d_{lat} = |V_{CP} - C_i'|. \quad (2)$$

To limit the distance d_{lat} , we use an euclidean length constraint d_{lat}^{max} . Once this threshold is reached, the attached skin node B_i is released, and the external force nulled with $\vec{f}_{B_i}^{ext} = 0$ to allow local skin relaxation. We got good results with heuristically estimated values for d_{lat}^{max} in the range between 2 cm to 4 cm. Finally, the lateral dragging force is computed:

$$\vec{f}_{B_i}^{lat} = \begin{cases} 0, & \text{if } (|\vec{f}_{n_i}| < f_{stick}) \vee (d_{lat} > d_{lat}^{max}) \\ (V_{CP} - C_i')k, & \text{if } (|\vec{f}_{n_i}| \geq f_{stick}). \end{cases} \quad (3)$$

```

1 for (each  $obj_i^{CD}$ )
2    $C_i, \vec{n}_i = \text{collision\_detection}(\vec{r}, obj_i^{CD});$ 
3   if ( $C_i \neq \text{NULL}$ ) // collision occurred
4     if ( $obj_i^{CD} \rightarrow \text{untouched}$ ) // first collision
5        $cp_i = \text{new constraint\_plane}(C_i, \vec{n}_i);$ 
6        $obj_i^{CD} \rightarrow \text{untouched} = \text{false};$ 
7     else // update collision contact
8        $cp_i \rightarrow \text{update}(C_i, \vec{n}_i);$ 
9        $\text{pulse\_force} \rightarrow \text{update}(T_{CP});$ 
10    if ( $obj_i^{CD} == \text{skin\_surface}$ ) // drag only skin
11       $|\vec{f}_{n_i}| = \text{calculate\_friction}(C_i, T_{CP});$ 
12      if (!dragging &&  $|\vec{f}_{n_i}| \geq f_{stick}$ ) // start dragging
13         $B_i = \text{proximity\_search}(V_{CP}, obj_j^B);$ 
14         $cs_i = \text{new constraint\_spring}(T_{CP}, B_i);$ 
15         $C'_i = C_i;$ 
16        dragging = true;
17      else // update dragging
18        if ( $|\vec{f}_{n_i}| \geq f_{stick}$ )
19           $cs_i \rightarrow \text{update}(T_{CP});$  //  $\vec{f}_{B_i}^{ext} = (V_{CP} - C'_i)k$ 
20           $d_{lat} = |V_{CP} - C'_i|;$ 
21          if ( $|\vec{f}_{n_i}| < f_{stick}$  ||  $d_{lat} > d_{lat}^{max}$ ) // stop dragging
22            delete  $cs_i;$  //  $\vec{f}_{B_i}^{ext} = 0$ 
23            dragging = false;
24          else
25            update_vishand( $C_i$ ); // constrained  $V_{CP} = C_i$ 
26        else // no collisions
27          delete  $cp_i;$ 
28           $obj_i^{CD} \rightarrow \text{untouched} = \text{true};$ 
29          update_vishand( $T_{CP}$ ); // unconstrained  $V_{CP} = T_{CP}$ 

```

Fig. 3. Pseudo-code for palpation simulation with visual coupling (Section 3.1), tissue dragging (Section 3.2), a multi-object force algorithm (Section 3.3), i.e., multiple cp_i , and a pulse force algorithm (Section 3.4) in a dynamic environment.

The normal and lateral dragging forces are combined and stored as force vectors in an external forcefield:

$$\vec{f}_{B_i}^{ext} = \vec{f}_{B_i}^n + \vec{f}_{B_i}^{lat} \quad (4)$$

This forcefield is applied to the nodes of a tetrahedral behavior mesh and thereby dragging and deforming the tissue. By using such behavior meshes our approach stays generic and can be utilized by mass-spring systems or finite element methods (FEM). In our case, a co-rotational FEM from SOFA [32] is used for the soft tissue simulation. In the pseudo code in Figure 3 we summarize the normal and lateral dragging force as a constraint spring cs_i , which approximates the influence of these forces by a spring between T_{CP} and B_i .

Subsurface structures are embedded in the behavior mesh either by barycentric mapping or by constraints applied to mesh nodes, e.g., fixed nodes that represent bones. Thus, internal structures like blood vessels are deformed accordingly if external dragging forces are acting on the skin surface.

3.3 Multi-Object Force Algorithm

For palpation of *subdermal structures*, i.e., objects under the skin layer, we use a multi-object force algorithm. A collision ray \vec{r} is attached to the unconstrained position of the input device T_{CP} , as explained already in visual coupling (see Section 3.1). On collision of \vec{r} with surface or subsurface objects, constraint planes are created (see Figure 5). The constraint plane cp_i is defined by the contact point of the collision C_i and a contact normal \vec{n}_i . Forces depend on the position of the haptic device T_{CP} relative to the constraint plane, i.e., the

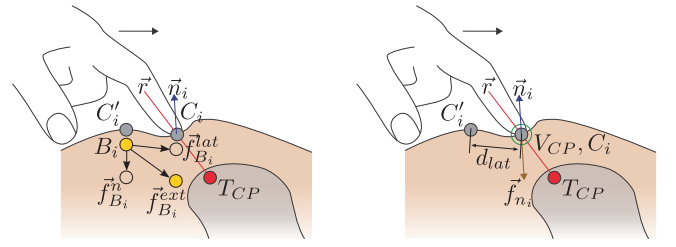


Fig. 4. Schematic overview of tissue dragging. B_i is the closest point in the behavior mesh obj_j^B to the first contact point C'_i . The point B_i is dragged by a force $\vec{f}_{B_i}^n$ in normal direction and by a force $\vec{f}_{B_i}^{lat}$ in lateral direction, which are combined to an external force $\vec{f}_{B_i}^{ext}$ (left). The distance d_{lat} between the initial contact point C'_i and the current V_{CP} and the magnitude of the force in normal direction \vec{f}_n determine the state of tissue dragging, i.e., stick or slip friction (right).

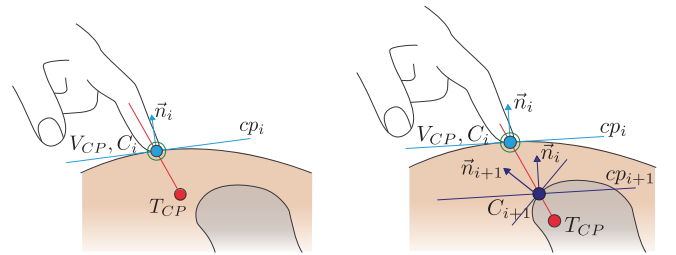


Fig. 5. Schematic overview of multi-object force rendering with one object in contact (left) and several objects with indirect contact (right). The light and dark blue lines representing constraint planes cp_i, cp_{i+1} for force feedback.

shortest distance Δd of T_{CP} to the constraint plane cp_i :

$$\Delta d = |\vec{n} \cdot (T_{CP} - C_i)|. \quad (5)$$

Then a haptic feedback force can be computed with Hooke's law, where k is a spring constant that is defined for each object/tissue type, and a damping term with a damping constant c and the device velocity is added to simulate viscosity:

$$\vec{f}_{cp_i} = k\Delta d\vec{n} + c\dot{T}_{CP}. \quad (6)$$

Both constants k and c have been adjusted for the simulation in expert reviews and depend on the limits and characteristics of the employed haptic device. The constraint planes in this approach are similar to the concept introduced for haptic rendering in [35], which supported one surface only. However, in our approach, the proxy-object V_{CP} has no history and utilizes no optimization algorithm. Instead, it is always moved to the outermost ray-intersection C_i , i.e., the virtual fingers stay on the skin surface and are consistent with the tissue dragging. Furthermore, the subsurface constraint planes are aligned with the surface plane, i.e., they are co-linear to the surface plane instead of being perpendicular to the local contact normal (e.g., dark blue continuous line compared to dashed line in Figure 5). We experimented with both alternatives and got more consistent and directional stable force output with the co-linear constraint planes.

Additionally, because the whole scene is dynamic, the force algorithm should be capable to perform haptic rendering of deformable objects. Not only the outermost surface is deformed by tissue dragging, but also the internal structures, embedded in the behavior mesh, are deformed accordingly. Therefore, to support the haptic rendering of deformable objects, the constraint planes are transformed accordingly during deformations. For example, the ligament in the hip region can be simultaneously deformed and "touched" by the palpating hand.

```

1 if (( $f_1 - f_0$ ) > (2 *  $f_{max}$ ))
2    $f_1 = f_0 + f_{max}$ ;
3 else if (( $f_1 - f_0$ ) >  $f_{max}$ )
4    $f_1 = (f_0 + f_1) / 2$ ;

```

Fig. 6. Pseudo-code to smooth forces, i.e., to prevent large discontinuities, between current force f_1 and previous force f_0 , as proposed by [18]. The algorithm is applied to all three force axes x, y, z separately.

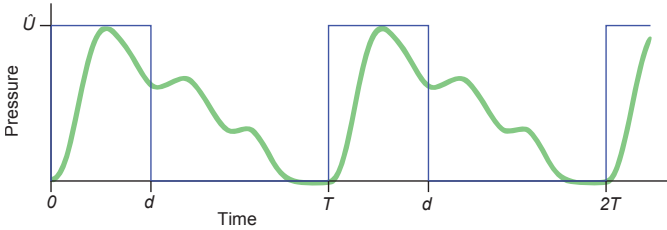


Fig. 7. A rectangular pulse wave (blue line) showing the pulse amplitude \hat{U} , duration d and period T , compared to a measured human arterial pulse signal (green line). The measured pulse form has been adapted from [38].

Force Interpolation and Smoothing

The positions and normals of the constraint planes are updated during the iterations of the palpation algorithm. Between such position updates (at 120 Hz), the force rendering algorithm evaluates the current haptic device position T_{CP} and calculates force vectors based on Hooke's law during the haptic render loop of the haptic device (at 1000 Hz). However, the switch between constraint planes, as well as low-resolution surface meshes, leads to discontinuities in the force output. To resolve this issue we combine two solutions. First, we use linear interpolation between constraint planes after each position update. Furthermore, we apply a special smoothing filter for force rendering [18]. This algorithm ensures a maximum force difference f_{max} between successive force frames f_0 and f_1 , as shown in Figure 6.

3.4 Pulse Force Algorithm

The human pulse is an important landmark for palpation and should be simulated with a force algorithm. We approximate the pulse signal with a rectangular wave form (see Figure 7). The duty cycle is defined as the ratio of the pulse duration d and pulse period T . To parametrize this wave form, we chose the following values: duty cycle $D = 0.2$, pulse rate $R = 50 - 160$ BPM (period $T = 1/R$) and peak amplitude $\hat{U} = 1$ N. These values are based on [38] and have been refined in expert reviews with our prototype. The pulse rate can be dynamically modified during the simulation, e.g., excitement of the virtual patient can be simulated by increased pulse rates.

Based on our previous work with a pulse simulation for particle-based soft tissue [40], we distribute pulse point sources P_i along the femoral artery. These pulse points have a predefined range r_{P_i} that represents the radius in which the pulse source can be felt. For optimal distribution, we recommend to place the pulse points with one radius distance between each other, e.g., utilizing a 3D modeling application. Thus, the intersecting volumes form a swept tube-like structure covering the artery (see Figure 8). One advantage of this approach is the fast collision detection with point-sphere tests, compared to more complex bounding volumes. Furthermore, these point sources are attached to the data structure of the femoral artery, which in turn is embedded in a behavior mesh. Thus, the pulse sources are modified and updated accordingly during tissue deformation, without costly operations, i.e., the update just consists of one barycentric transform for each pulse source point. Pulse forces are calculated when the tool center point of the haptic device T_{CP} is within range of a pulse point

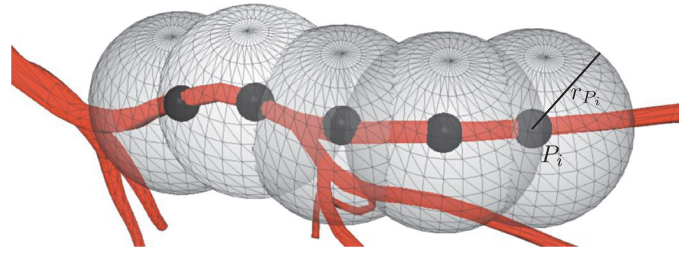


Fig. 8. Example of arterial pulse point sources P_i with influence ranges r_{P_i} .

sources $\Delta d \leq r_{P_i}$, where:

$$\Delta d = |P_i - T_{CP}|. \quad (7)$$

Thus, the pulsating force is computed depending on distance and simulation time:

$$\vec{f}_{P_i}(t) = \begin{cases} 0, & \text{if } (d < (t \bmod T)) \vee (\Delta d > r_{P_i}) \\ k(r_{P_i} - \Delta d)\vec{n}, & \text{if } (t \bmod T) \leq d. \end{cases} \quad (8)$$

The stiffness constant k which equals to \hat{U} can be varied to model low or high blood pressure. The force direction depends on \vec{n} , which can be defined as the normalized vector between T_{CP} and P_i . However, we suggest to use the contact normal of the surface for \vec{n} , in order to have a more directional consistent force output over time. Furthermore, the inverse relationship of the force magnitude to the difference between distance Δd and range r_{P_i} of the pulse points creates a very subtle pulse force that gets stronger with closer proximity.

4 PALPATION PAD

In order to improve the user interface for the palpation task, we propose an easy-to-replicate modification of the hardware of the PHANTOM Omni haptic device. Several approaches have been already reported, which replace the default stylus of the haptic device with a finger thimble for palpation [5, 42, 23]. One similarity between these solutions is that the tip of the index finger is inserted into a finger thimble. However, for the palpation task at least two fingers should interact with the simulated surface. Although, multiple haptic devices could be used to support haptic feedback of several fingers, e.g., three haptic devices have been combined to support grasping tasks [29], we opted for a solution with a single device. The problem with multiple devices for one hand is the overlap of workspaces which limits close alignment of fingers and furthermore increased costs of several devices.

In order to design this new extension, we first collected technical and medical requirements. From a technical point of view, the extension should be light weight, e.g., the default stylus weighs 25 g. To attach the new extension, a female 1/4" jack plug should be used, because this standardized connector type is already used for the default stylus. Application-based requirements, i.e., based on the medical procedure of palpation, are a non-prehensile grip and a hand-pose with extended index and middle finger, where only the finger tips are in contact with the device. In comparison, the stylus requires a prehensile grip including the thumb, which contradicts the requirements for palpation where the thumb should not be in contact with the device. The device extension was constructed in a user-centered design process. Several prototypes were iteratively tested and refined with three subject matter experts: one anatomy professor, one veterinarian, who has to rely strongly on palpation, and an anesthesiologist with regional anesthesia experience.

We have opted for a pad shape, to enable a natural control interface with a palpation finger posture. The pad is operated with the distal segments (fingertips) of the index and middle fingers strapped onto the pad's surface by rubber bands. The design was optimized to be lightweight while still maintaining stability and durability. Furthermore, the size and shape of the pad have been adjusted for average

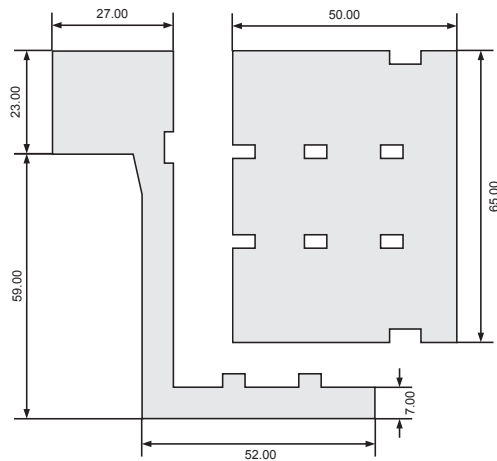


Fig. 9. Cutting plan for the palpation pad from 3 mm acrylic glass: side part (left) needed twice and one base plate (right).

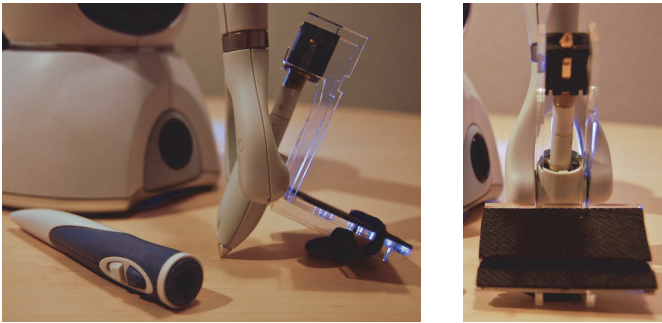


Fig. 10. Side (left) and front view (right) of the palpation pad attached to the PHANTOM Omni haptic device. The pad is aligned closely to the rotation center of the device's end effector to improve stability.

finger sizes. The construction was assembled from 3 mm acrylic glass laser-cut shapes (see Figure 9) and equipped with a 1/4" jack plug to connect to the end effector of the device (see Figure 10). Standard 3 mm thick foam rubber with an adhesive backside was used to provide a neutral surface material. This material was chosen by the subject matter experts and their preferred choice because of the grip/friction and neutral temperature properties (warms up quickly to the finger contact). The material was compared to pure acrylic glass surface ("too artificial"), to thin latex material ("too slippery on the acrylic glass surface") and to thin silicon material ("too soft"). The complete extension weighs 30 g. Thinner versions turned out to be too fragile. Because of this very minor weight difference to the default stylus, we added no gravity compensation to the force rendering algorithms. An example of the usage of this device extension is shown in Figure 1.

5 USER STUDY

5.1 Experiment Design

The experiment design employs an expert review for face validation of a simulator prototype that utilizes the palpation interaction and the palpation pad described in the previous two sections. The participants were first introduced to the simulator and given five minutes to familiarize themselves with the controls. Then, they were tasked to find the femoral pulse in the inguinal region and to insert the needle next to it, to reach as close as possible to the nervus femoralis, with an upper time limit of ten minutes. Only one dataset was used and the main goal during the task was set on evaluating the haptic feedback and soft tissue simulation and not on a successful outcome of the procedure. An additional task was introduced to compare the custom-built palpation pad (see Section 4) with the default stylus of the haptic device.

Therefore, after completing the first task, the end effector of the haptic device for the palpation hand was exchanged by the default stylus. Then, the users were asked to try out palpation for a few more minutes with this changed hardware. The user study was carried out with a group of anesthesiologists at the local university hospital over a time span of two weeks.

5.2 Apparatus

The apparatus for this user study consists of two haptic devices (PHANTOM Omni[®] haptic device, SensAble Technologies), a passive-stereo VR-desktop system with a SXGA+ 60" rear-projection screen (flip_150, imsys) coupled with an optical IR-tracking system (TrackPack, Advanced Realtime Tracking) and is driven by a 2.4 GHz (Intel[®] Core[™]2 Quad) desktop PC with 4 GB RAM, Windows 7 operating system and a Quadro FX 4600 graphics card with 768 MB RAM (Nvidia). The haptic devices were positioned and fixed 27 cm apart (center to center) on a height-adjustable rack (bottom plate to floor: 78–104 cm) that was located in front of the screen (see Figure 1, right). The devices were operated in a standing position.

5.3 Software

The prototype allows for bimanual interaction and has components for a physics-based FEM soft tissue simulation, interaction algorithms utilizing collision detection and visual and haptic rendering. The update rates were set for the two haptic loops to 1000 Hz, for simulation to 25 Hz, for interaction and collision detection of each hand to 120 Hz respectively and to maximal possible visual frame rate, which reached on average 70 Hz. A detailed description of the system architecture can be found in [41]. Here, the main goal of this prototype is to provide a system for evaluation of the palpation interaction and haptic rendering. The femoral block technique from regional anesthesia has been chosen as an example application scenario [19, 39]. The virtual patient's exposed inguinal region and the instruments are visualized. Additionally, virtual shadows have been added to improve depth perception and a skin shader was implemented. A volumetric mesh has been created for the co-rotational FEM-based soft tissue simulation and consists of approximately 2000 tetrahedra and covers the needle insertion and palpation area in the hip region. Additional surface meshes represent different anatomical layers and are linked with barycentric mappings to deformations of the soft tissue volumetric mesh. The interaction is bimanual, i.e., palpation and needle insertion can be performed simultaneously. A virtual hand for palpation can be intuitively controlled with a modified haptic device, as described in Section 4. The hand can be used to interact visually and haptically with the skin surface and internal anatomical structures of the virtual patient, as described in Section 3. With a similar haptic device, using a different handle, a virtual needle can be controlled. The needle can be used to puncture several anatomical layers and interact visually and haptically with the according soft and hard tissue structures.

For the femoral block, the first task is to localize anatomical landmarks, e.g., the hip bone, ligament and femoral pulse, to determine an insertion site for the needle. To perform this task with palpation, a virtual hand with two extended fingers, i.e., index and middle finger as a "sensor", can touch and interact with the skin surface of the virtual patient (see Figure 1) via a haptic device. On collision, the skin can be deformed or dragged and anatomical landmarks can be perceived with haptic feedback, as described in Section 3. As soon as a particular puncture site has been chosen, the needle can be inserted as a second task, which is controlled by the other hand. During the insertion, the palpation hand can be used for guidance and is usually kept on top of the femoral artery location.

5.4 Measures, Error Metrics & Questionnaire

We prepared a post-test questionnaire with a 7-point Likert scale (1 = strongly agree, to 7 = strongly disagree). The items were grouped into controls and interface, visuals, simulation, haptics of the simulator, acceptance and detailed questions about the palpation pad and palpation interaction. An overview of the items follows in the results section.

Table 1. Overview of demographics and experience of the two groups for the face validation of the simulator prototype ($N_{G1} = 23$ and $N_{G2} = 17$). Abbreviations: RA = any kind of RA procedure, FB = femoral block, Mean \pm SD.

D	Item	G1	G2
1	Age (years)	30.9 \pm 3.52	40.0 \pm 6.64
2	Work (years)	2.9 \pm 2.13	12.4 \pm 6.62
3	Gender	σ : 10; φ : 13	σ : 13; φ : 4
4	Handedness (right)	86.9%	94.1%
5	Palpation (daily)	60.8%	76.5%
6	Needle (daily)	60.8%	76.5%
7	RA (\geq weekly)	17.3%	58.8%
8	Total amount of RA	41.2 \pm 41.3	447.5 \pm 323.9
9	FB (\geq monthly)	43.4%	82.4%
10	Total amount of FB	7.9 \pm 8.3	60.2 \pm 62.7
11	VR Simulator (\geq weekly)	0%	0%
12	Video Games (\geq weekly)	13.1%	23.5%

Furthermore, the participants were informally interviewed afterwards to provide additional feedback.

5.5 Participants

The participants have been divided into two groups $G1$ and $G2$. $G1$ consists of 23 beginners, i.e., residents, from a clinic for anesthesiology. All individuals in this group have less than five years of work experience. The group $G2$ consists of 17 experts, i.e., consultants and attendings. The subjects of this second group are anesthesiologists from the same clinic and have at least five years of work experience per subject. All participants were asked for their age, gender, handedness, work experience and specific experience in the medical domain with palpation and needle procedures, and experience in the technical domain with VR-based simulators and video games (see Table 1).

5.6 Results

The results of the questionnaire are summarized for both groups in Table 2. Color coding has been added to visualize how positive or negative the results have been. While in summary results are not strongly positive, there are only few negative results. In the following, the results are analyzed statistically in more detail.

Comparison between Groups

The answers of the questionnaire have been compared between groups by non-parametric tests. Pair-wise Mann-Whitney U tests have been conducted for all questionnaire items to screen between groups for dissimilarities. On average the haptics for the right hand (needle interaction) have been perceived significantly more stable (Q20) by $G2$ ($M = 2.2$, $SE = 0.38$) than by $G1$ ($M = 3.6$, $SE = 0.38$), $U = 106.0$, $p < .05$, $r = -.39$. Besides this one exception, there were no significant differences found between the medical beginners and experts.

Comparison between Pad and Stylus

As mentioned in Section 5.1, both groups performed an additional task to compare the palpation pad to a default stylus. Because this was a within-subject design, paired (dependent) t-tests were performed to compare the according questionnaire items between palpation pad and default stylus. The results are summarized in Table 3. In both groups, natural interaction (Q1 vs. Q5) and fitting HW (Q2 vs. Q6) have been significantly rated in favor of the pad. Furthermore, though not significant, the items (Q3 vs. Q7) and (Q4 vs. Q8) are on average better for the pad.

Correlations

Finally, we computed Pearson's correlation coefficient in a matrix comparing all the demographic, experience and questionnaire items from Tables 1 and 2. The most significant correlation pairs are summarized in Table 4.

Table 2. Results of the post-test questionnaire (7-point Likert scale: 1 = strongly agree, to 7 = strongly disagree; items with an asterisk (*) have a 3-point scale: -1 = too weak, 0 = OK, +1 = too strong). Left palpation hand (LH), right needle hand (RH) and hardware (HW). Color coding: positive = green, neutral = yellow and negative = red.

Q	Item	G1		G2	
		M	SD	M	SD
1	Natural interaction LH Pad	3.3	1.75	3.2	1.52
2	Fitting HW LH Pad	3.2	1.68	3.1	1.93
3	Not tiring LH Pad	2.8	1.78	2.5	1.51
4	No problems interaction LH Pad	4.0	2.02	3.6	1.97
5	Natural interaction LH Stylus	4.8	1.72	4.8	1.51
6	Fitting HW LH Stylus	5.1	1.73	5.3	1.61
7	Not tiring LH Stylus	3.6	1.83	2.7	1.72
8	No problems interaction LH Stylus	4.8	1.68	4.6	2
9	Natural interaction RH	2.9	1.58	3.0	1.58
10	Fitting HW RH	3.0	1.77	2.5	1.81
11	Not tiring RH	2.3	1.6	1.6	0.8
12	No problems interaction RH	3.0	2.11	2.5	1.77
13	Visuals realistic	3.0	1.51	2.7	1.05
14	Tissue deforms realistic	4.1	1.56	4.2	1.64
15	Haptics realistic LH	3.7	1.45	3.9	1.62
16	Stiffness plausible LH	3.6	1.56	3.9	1.69
17	Stable haptics LH	3.4	1.99	3.9	2.44
18	Haptics realistic RH	3.5	1.97	3.1	1.95
19	Stiffness plausible RH	3.1	1.68	3.1	1.6
20	Stable haptics RH	3.6	1.83	2.2	1.56
21	Natural fingerpos on Pad	3.3	1.57	3.8	1.82
22	Sufficient range of Pad	3.3	1.97	3.1	2.02
23	Stable control of Pad	3.4	1.88	3.0	1.95
24	Neutral material on Pad	2.9	1.88	1.9	0.67
25	Pulse simulation realistic	3.7	1.78	3.0	1.81
26	Pulse magnitude(*)	0.4	0.61	0.2	0.58
27	Pulse position	4.3	1.53	3.8	1.91
28	Skin resistance realistic	4.5	1.38	3.8	1.75
29	Skin resistance magnitude(*)	-0.4	0.78	-0.8	0.45
30	Skin deforms realistic	4.2	1.52	4.6	1.88
31	Skin deformation magnitude(*)	-0.6	0.7	-0.5	0.69

Comments and Observations

After the post-test questionnaires all subjects were asked for additional feedback. We have collected and categorized this feedback into comments about the simulator application and comments about the hardware. Within the context of the simulator application, several suggestions were made about the virtual fingers: approximately 15% of all participants suggested to align the finger tips of the palpation hand (see Figure 11), 7% requested to spread fingers of the palpation hand to insert the needle in-between, and one subject remarked that the finger nails of the virtual model should be shortened for palpation. The virtual arms were sometimes occluding the view for approximately 9% of the subjects. Suggestions were made about the simulator environment, e.g., to create a model of the operating room, to add blood on puncture, to provide oral feedback from the patient (pain screams), and to allow different positions relative to the virtual patient, e.g., view from the top, or standing slightly rotated. A few subjects would have preferred to switch hands during the procedure, e.g., palpate with dominant hand and switch to needle later. Looking at the feedback about the hardware interface, most comments related to the pad: building different sizes to accommodate bigger and smaller fingers, contradicting opinions between subjects about the surface to make it either smoother or to add more grip, 12% of the subjects requested to have more contact with finger tips on the pad, some participants would have preferred to put the fingers perpendicular to the surface on the pad, and one person suggested to give individual tactile feedback for each fingertip. Only one person requested a co-located setup of hardware input and virtual arms display. In general, even subjects who gave only average ratings to the simulator, stated that they could see a benefit in the simulator.

During the user study we observed the behavior and reactions of the

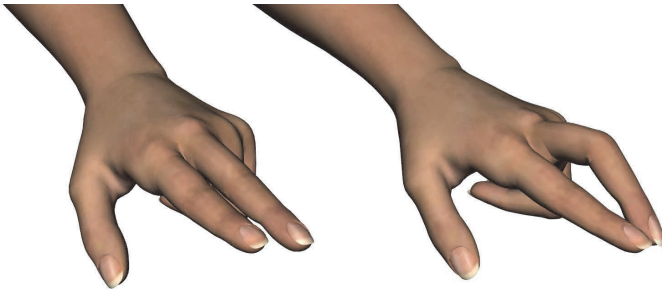


Fig. 11. Variations of palpation hand: stretched fingers used for the user study (left), aligned fingertips, as suggested during the user study (right).

test subjects. Several subjects were really intrigued by the simulator and gave very positive feedback. Some participants felt uncomfortable with the hardware interface. However, it was also observed that most subjects quickly got used to the controls and thus the training phase should be adjusted individually.

5.7 Discussion

Differences between Groups

The significant differences for (Q20) can probably be explained by better dexterity with more work experience, consequently making the needle interaction fluent and “effortless”. Although, no other significant differences could be found between the two groups, at least some notable differences on average have been found. For example, on average group *G2* rated palpation and especially pulse realism better (Q25-Q28) compared to group *G1*, which might be also explainable by higher work and palpation experience.

Pad Hardware Extension for Palpation

The pad received many comments and suggestions for improvement. Although expert reviews had been conducted during the development of the pad, it appears that the requirements are rather subjective and cannot be easily generalized. Therefore, it is probably best to create several variations of the pad to meet different personal preferences. Due to the low costs of production this seems to be feasible. In conclusion, though the palpation pad is still far from perfect, it seems to be already a strong improvement over the default stylus.

Explanation of Correlations

The pairs (C1) and (C2) from Table 4 let us assume that the interaction with the stylus appears to be more natural with higher age and the finger position on the pad feels less natural. (C1) might be explainable by the fact that medical experts are more used to indirect interaction and additionally some attendings preferred the finger tip’s positions on the stylus over the pad because of a higher amount of sensitive contact. The inverse relationship between age and natural rated finger position on the pad (C2) can be also explained by user comments about the finger’s position. (C3) suggests that with more palpation experience the surface of the Pad is perceived to be less distracting. However, the pulse magnitude was perceived to be a bit too strong with more palpation experience as shown in (C4). Natural interaction of the palpation pad correlates positively with other items to rate the pad: fitting HW (C5), natural finger position on pad (C6), sufficient range of pad (C7) and stable control of pad (C8). According to the correlation coefficients, visual realism depends on tissue deformation (C9) and skin deformation (C10). Interestingly, we found a strongly significant correlation between realistic tissue deformation and realistic haptics for LH (C11) and plausible stiffness for LH (C12). Furthermore, realistic tissue deformation correlates with realistic skin resistance (C13). These last three correlations indicate the strong relationship between perceived realism between different modalities. That is to say, the visual quality of the physics-based soft tissue simulation appears to influence the kinesthetic perception. Plausible stiffness of LH correlates

to realistic skin resistance (C14), which are strongly related and like control questions to each other.

Comparison to Non-Virtual Simulators

Medical simulation is often associated with full-scale simulator mannequins rather than virtual reality-based simulators. There are several commercial solutions, e.g., from Laerdal Medical and CAE Healthcare, with many workshops and simulator groups. In most cases these simulators are focused on global anesthesia and intensive care which revolves around simulations of drugs, external live support and several physiological systems. Subsequently, in the user study we also got comparative feedback from several subjects that have been working with such full-scale simulators before. Most of these comments were subjected towards the hardware interface, and questions were asked if the input devices could be replaced by something less intimidating. However, one has to keep in mind that most subjects never saw a haptics device before and after some training got used to it. Nevertheless, there are some alternatives. One option is to co-locate the visual and haptic feedback with a mirror and thereby shielding the haptic device from the users view, or another option is to use a head-mounted display. However, these systems can be also intimidating to a non-technical user and could be potentially non-ergonomic for longer training sessions. Future work could focus on a fusion of prop-based simulators and virtual reality, which has been also already done by some groups with augmented reality-based prototypes. Furthermore, there are so-called skills trainer modules, e.g., rubber limbs that are used for needle insertion training or silicon-/gel-based breast models with artificial lumps inside for cancer palpation training. While these solutions can provide high tactile realism, they are prone to material deterioration from repeated use. Furthermore, modifications of scenarios and performance metrics are more difficult to implement than with VR-based approaches. For palpation in particular, VR-based approaches are better in our opinion, because of full control over the environment and many potential extensions, e.g., a teacher could connect with an additional haptic device to feel the forces that the trainee is encountering or a guiding force can be recorded to convey what should be felt.

Hardware Limitations

Depending on the type of palpation three degrees of freedom (DOF) for the input and force output or even less can be enough. [28] identified and classified several kinds of *hand exploratory procedures*, e.g., to sense texture, lateral motions are used and to sense stiffness, pressure is applied. A taxonomy for palpation [34] made further distinctions for medical procedures based on observations and related classifications. 3 DOF movement should be sufficient for the palpation procedure that we chose for the user study. Nevertheless, torque output from 6 DOF force feedback devices might be helpful in certain occasions and could be investigated in future work by a comparative study. The low maximum stiffness of the used haptic hardware devices (PHANTOM Omni) is a bigger issue. During the user study, we often observed that some participants tried to increase pressure on the device, if they could not find any pulse. Longer durations of high stiffness led to overheating of the devices and also limited the maximum pressure that participants could apply. Other devices that can output stronger forces are often very expensive or have higher back drive friction. This trade-off between precision and high stiffness should be always considered. To the best of our knowledge there is no optimal solution yet, although new devices are under development by several research groups and companies. Another concern before our first tests was the supported frequency and fidelity of the haptic device for pulse simulation. Usually, the pulse is simulated with special tactile actuators and not with kinesthetic devices such as the PHANTOM Omni device. However, initial tests gave a plausible and if needed very subtle pulse sensation which has been also confirmed by the results of the user study. Still, in ongoing work of other research groups haptic devices are improved and combinations of tactile devices mounted on kinesthetic devices are developed that could also be applied in the future for palpation interaction.

Table 3. Within-subject comparison for group $G1$ and $G2$ between Pad and stylus (Q 1-4 and 5-8 from Table 2 respectively) with paired t-test.

Q	Item	$G1$ t-test		$G2$ t-test	
		t(22)	p	t(16)	p
1 vs. 5	Natural interaction	-2.615	.016	-3.7	.002
2 vs. 6	Fitting HW	-2.955	.007	-3.816	.002
3 vs. 7	Not tiring	-1.779	.089	-0.347	.733
4 vs. 8	No problems interaction	-1.351	.191	-1.247	.230

Table 4. Pairs with significant Pearson's correlation coefficient r over all groups.

C	Item 1	Item 2	N	r	p
1	Age (D1)	Natural interaction LH Stylus (Q5)	40	-0.32	.044
2	Age (D1)	Natural fingerpos Pad (Q21)	38	0.32	.048
3	Palpitation experience (D5)	Neutral material Pad (Q24)	38	-0.37	.021
4	Palpitation experience (D5)	Pulse magnitude (Q26)	38	0.32	.047
5	Natural interaction LH Pad	Fitting HW LH Pad	49	0.53	.000
6	Natural interaction LH Pad	Natural fingerpos on Pad	38	0.48	.002
7	Natural interaction LH Pad	Sufficient range of Pad	38	0.34	.037
8	Natural interaction LH Pad	Stable control of Pad	38	0.37	.023
9	Visuals realistic	Tissue deforms real.	49	0.45	.001
10	Visuals realistic	Skin deforms realistic	38	0.36	.026
11	Tissue deforms real.	Haptics realistic LH	49	0.65	.000
12	Tissue deforms real.	Stiffness plausible LH	49	0.59	.000
13	Tissue deforms real.	Skin resistance realistic	38	0.33	.046
14	Stiffness plausible LH	Skin resistance realistic	38	0.38	.018

Plausibility of Palpation Interaction

It is of course always difficult to rate subjective measures. However, with the comparisons between groups and the correlation analysis we tried to filter for individual levels of experience. While we did not analyze each component of the palpation interaction algorithm separately, in combination they seem to deliver acceptable results for the simulation. We want to emphasize on the difference between plausibility (sufficient for procedural training) and high realism (required for patient-specific rehearsal). From the aforementioned results and discussions we conclude that the palpation interaction is reasonably plausible for the medical task that was simulated by the prototype.

Lessons Learned

While the overall acceptance of the simulator got mostly positive ratings, there were also some participants with mixed reviews, e.g., problems with the controls. Probably, for such individuals, it might help to conceal the hardware devices, e.g., either with a mixed reality setup or a co-located haptic interface. Nevertheless, the palpation pad already turned out to be a good improvement, in comparison to the default stylus of the haptic device. Furthermore, we observed that some test subjects needed a longer time to get used to the system. Therefore, the time to learn how to control the simulator should be adjusted individually. Ultimately, the system should feel as natural as possible and be usable without prior training. In conclusion, the pulse simulation was rated very well, the needle simulation plausible and the tissue deformation also plausible but slightly too weak, i.e., there was too little indentation in normal direction.

6 CONCLUSION

In this paper, we have proposed a novel palpation interaction approach and provided a detailed description of an extensive user study about this approach. One of the key differences of our approach to the related work on palpation, is the tissue dragging algorithm. Most approaches employ a penalty-based collision interaction between a rigid body (palpation hand) and a soft body surface (soft tissue). In comparison, our approach utilizes friction to calculate external forces for tissue dragging based on friction. Additionally, in our case the proximity search and tissue dragging instead of a collision-based deformation avoids pop-through artifacts. Furthermore implementations of a multi-object force algorithm and a pulse force algorithm are described, which create plausible haptic effects needed for kinesthetic identification of subsurface structures. To improve the haptic device, we proposed a novel lightweight palpation pad. This hardware extension is easy to construct and showed significantly better ratings in the user study than the default stylus of the haptic device.

As the main contribution of this article, a large user study with medical experts has been described. For this purpose we integrated the proposed algorithms into a medical simulator prototype. The results of the user study have been analyzed, discussed in detail and provide helpful insights for the design and implementation of similar virtual reality-based medical simulators and palpation interaction approaches.

Future work could focus on the improvement of the haptic hardware interface, e.g., multi-finger haptic devices would be beneficial, but should be reduced in costs, be less intrusive and have less constrained workspaces. For cutaneous sensation of dragging and pulse feedback, tactile actuators could be positioned on the palpation pad at the location of the user's fingertips.

While the results of this paper contribute primarily to palpation for medical training simulators, the interaction approach and simulation could be also applied for generic haptic interaction with rigid or deformable objects in virtual environments. In conclusion, the haptic palpation with the simulated deformable tissue and the hardware extension was rated mostly positively by medical experts.

ACKNOWLEDGMENTS

The authors wish to thank their coworkers and students, in particular Bernd Hentschel, Thomas Knott, Yuen Law, Dominik Rausch and Daniel Kneer, the medical advisors Prof. Rolf Rossaint, Sadie Behrens, Oliver Grottko, Andreas Herrler, Stephan Macko and Prof. Andreas Prescher, and the participants of the user study from the staff of the Department of Anaesthesiology, RWTH Aachen University Hospital. This work was funded by the German Research Foundation (project IDs: 19576470 and 80893132 at <http://gepris.dfg.de>).

REFERENCES

- [1] E. Acosta, B. Stephens, B. Temkin, J. A. Griswold, S. A. Deeb, T. M. Krummel, and P. J. Gorman. Development of a haptic virtual environment. In *CBMS '99: Proceedings of the 12th IEEE Symposium on Computer-Based Medical Systems*, pages 35–39, Washington, DC, USA, 1999. IEEE Computer Society.
- [2] M. O. Alhalabi, V. Daniulaitis, H. Kawasaki, and T. Hori. Medical training simulation for palpation of subsurface tumor using HIRO. In *First Joint Eurohaptics Conference, 2005 and Symposium on Haptic Interfaces for Virtual Environment and Teleoperator Systems, 2005. World Haptics 2005.*, pages 623–624, March 2005.
- [3] B. Armstrong-Hélouvy, P. Dupont, and C. Canudas de Wit. A survey of models, analysis tools and compensation methods for the control of machines with friction. *Automatica*, 30:1083–1138, July 1994.
- [4] S. Baillie, A. Crossan, S. Brewster, D. Mellor, and S. Reid. Validation of a bovine rectal palpation simulator for training veterinary students. *Studies in Health Technology and Informatics*, 111:33–36, 2005.
- [5] S. Baillie, A. Crossan, S. Reid, and S. Brewster. Preliminary Development and Evaluation of a Bovine Rectal Palpation Simulator for Training Veterinary Students. *Journal of Cattle Practice*, 11(2):101–106, 2003.
- [6] G. Burdea, G. Patounakis, V. Popescu, and R. E. Weiss. Virtual reality-based training for the diagnosis of prostate cancer. *Biomedical Engineering, IEEE Transactions on*, 46(10):1253–1260, October 1999.

- [7] E. Burns, S. Razaque, M. C. Whitton, and F. P. Brooks. MACBETH: Management of Avatar Conflict by Employment of a Technique Hybrid. *The International Journal of Virtual Reality*, 6(2):11–20, 2007.
- [8] H. Chen, W. Wu, H. Sun, and P.-A. Heng. Dynamic touch-enabled virtual palpation. *Computer Animation and Virtual Worlds*, 18(4-5):339–348, September 2007.
- [9] T. Coles, N. W. John, D. A. Gould, and D. G. Caldwell. Haptic Palpation for the Femoral Pulse in Virtual Interventional Radiology. In *Second International Conferences on Advances in Computer-Human Interactions, 2009. ACHI '09.*, pages 193–198, February 2009.
- [10] T. R. Coles, D. A. Gould, N. W. John, and D. G. Caldwell. Virtual Femoral Palpation Simulation for Interventional Radiology Training (Work in Progress Paper). In *EG UK Theory and Practice of Computer Graphics*, pages 123–126, 2010.
- [11] J. Colgate, M. Stanley, and J. Brown. Issues in the haptic display of tool use. In *International Conference on Intelligent Robots and Systems*, volume 3, pages 140–145, 1995.
- [12] A. Crossan, S. Brewster, S. Reid, and D. Mellor. A horse ovary palpation simulator for veterinary training. In S. Brewster and R. Murray-Smith, editors, *Haptic Human-Computer Interaction*, volume 2058 of *Lecture Notes in Computer Science*, pages 157–164, Berlin, Heidelberg, July 2001. Springer Berlin Heidelberg.
- [13] V. Daniulaitis, M. O. Alhalabi, H. Kawasaki, Y. Tanaka, and T. Hori. Medical palpation of deformable tissue using physics-based model for haptic interface robot (HIRO). In *Proceedings of 2004 IEEE/RSJ International Conference on Intelligent Robots and Systems*, pages 3907–3911, 2004.
- [14] M. Dinsmore, N. Langrana, G. Burdea, and J. Ladeji. Virtual reality training simulation for palpation of subsurface tumors. In *Proceedings of the 1997 Virtual Reality Annual International Symposium (VRAIS '97)*, pages 54–60, March 1997.
- [15] T. Endo, H. Kawasaki, T. Mouri, Y. Doi, T. Yoshida, Y. Ishigure, H. Shimomura, M. Matsumura, and K. Koketsu. Five-fingered haptic interface robot: HIRO III. In *Proceedings of the World Haptics 2009 - Third Joint EuroHaptics conference and Symposium on Haptic Interfaces for Virtual Environment and Teleoperator Systems*, pages 458–463, Washington, DC, USA, 2009. IEEE Computer Society.
- [16] G. J. Gerling and G. W. Thomas. Augmented, Pulsating Tactile Feedback Facilitates Simulator Training of Clinical Breast Examinations. *Human Factors: The Journal of the Human Factors and Ergonomics Society*, 47(3):670–681, January 2005.
- [17] D. Gomez, G. Burdea, and N. Langrana. Integration of the Rutgers Master II in a virtual reality simulation. In *VRAIS '95: Proceedings of the Virtual Reality Annual International Symposium*, pages 198–202, 1995.
- [18] A. Gregory, A. Mascarenhas, S. Ehmann, M. Lin, and D. Manocha. Six Degree-of-Freedom Haptic Display of Polygonal Models. In *the IEEE Visualization*, pages 139–146, 2000.
- [19] O. Grottko, A. Ntoubas, S. Ullrich, W. Liao, E. Fried, A. Prescher, T. M. Deserno, T. Kuhlen, and R. Rossaint. Virtual reality-based simulator for training in regional anaesthesia. *British Journal of Anaesthesia*, 103(4):594–600, October 2009.
- [20] H.-Y. Han, A. Shimada, and S. Kawamura. Analysis of friction on human fingers and design of artificial fingers. In *IEEE International Conference on Robotics and Automation*, volume 4, pages 3061–3066, Apr. 1996.
- [21] D. Karnopp. Computer Simulation of Stick-Slip Friction in Mechanical Dynamic Systems. *Journal of Dynamic Systems, Measurement, and Control*, 107(1):100–103, 1985.
- [22] H. Kawasaki, J. Takai, Y. Tanaka, C. Mrad, and T. Mouri. Control of multi-fingered haptic interface opposite to human hand. In *Proceedings of the 2003 IEEE/RSJ Intl. Conference on Intelligent Robots and Systems*, pages 2707–2712, 2003.
- [23] K. J. Kuchenbecker, D. Ferguson, M. Kutzer, M. Moses, and A. M. Okamura. The Touch Thimble: Providing Fingertip Contact Feedback During Point-Force Haptic Interaction. In *HAPTICS '08: Proceedings of the 2008 Symposium on Haptic Interfaces for Virtual Environment and Teleoperator Systems*, pages 239–246, Washington, DC, USA, 2008. IEEE Computer Society.
- [24] Y. Kuroda, M. Nakao, T. Kuroda, H. Oyama, M. Komori, and T. Matsuda. FEM-based interaction model between elastic objects for indirect palpation simulator. *Studies in Health Technology and Informatics*, 98:183–189, 2004.
- [25] K.-U. Kyung, J. Park, D.-S. Kwon, and S.-Y. Kim. Real-Time Area-Based Haptic Rendering for a Palpation Simulator. In M. Harders and G. Székely, editors, *Biomedical Simulation*, volume 4072, chapter 15, pages 132–141. Springer Berlin Heidelberg, Berlin, Heidelberg, 2006.
- [26] L. D. Landau and E. M. Lifshitz. *Theory of elasticity*, chapter Solid Bodies in Contact, pages 26–31. Butterworth-Heinemann, 3rd edition, 1986.
- [27] N. A. Langrana, G. Burdea, K. Lange, D. Gomez, and S. Deshpande. Dynamic force feedback in a virtual knee palpation. *Journal of Artificial Intelligence in Medicine*, 6(4):321–333, August 1994.
- [28] S. J. Lederman and R. L. Klatzky. Hand movements: A window into haptic object recognition. *Cognitive Psychology*, 19(3):342–368, July 1987.
- [29] S. McKnight, N. Melder, A. Barrow, W. Harwin, and J. Wann. Psychophysical Size Discrimination using Multi-fingered Haptic Interfaces. In *Proceedings of Eurohaptics*, pages 274–281, 1994.
- [30] A. Nahvi, J. M. Hollerbach, R. Freier, and D. D. Nelson. Display Of Friction In Virtual Environments Based On Human Finger Pad Characteristics. In *Proc. ASME Dynamic Systems and Control Division*, pages 179–184, 1998.
- [31] J. R. Napier. The prehensile movements of the human hand. *The Journal of Bone and Joint Surgery*, 38-B:902–913, Nov 1956.
- [32] M. Nesme, Y. Payan, and F. Faure. Efficient, Physically Plausible Finite Elements. In J. Dingliana and F. Ganovelli, editors, *Eurographics*, pages 77–80, August 2005.
- [33] R. Parkes, N. Forrest, and S. Baillie. A mixed reality simulator for feline abdominal palpation training in veterinary medicine. *Studies in health technology and informatics*, 142:244–246, 2009.
- [34] W. J. Peine. *Remote Palpation Instruments for Minimally Invasive Surgery*. PhD thesis, Harvard University, 1999.
- [35] D. C. Ruspini, K. Kolarov, and O. Khatib. The haptic display of complex graphical environments. In *SIGGRAPH '97: Proceedings of the 24th annual conference on Computer graphics and interactive techniques*, pages 345–352, New York, NY, USA, 1997. ACM Press.
- [36] A. V. Savescu, M. L. Latash, and V. M. Zatsiorsky. A technique to determine friction at the fingertips. *Journal of Applied Biomechanics*, 24:43–50, Feb 2008.
- [37] G. Schwarz, G. Feigl, R. Kleinert, C. Dorn, G. Litscher, A. Sandner-Kiesling, and N. Bock. Pneumatic pulse simulation for teaching peripheral plexus blocks in cadavers. *Anesthesia & Analgesia*, 95(6):1822–1823, 2002.
- [38] P.-H. Tsui, L.-Y. Lin, C.-C. Chang, J.-J. Hwang, J.-J. Lin, C.-C. Chu, C.-N. Chen, K.-J. Chang, and C.-C. Chang. Arterial pulse waveform analysis by the probability distribution of amplitude. *Physiological Measurement*, 8(8):803–812, July 2007.
- [39] S. Ullrich, O. Grottko, E. Fried, T. Frommen, W. Liao, R. Rossaint, T. Kuhlen, and T. M. Deserno. An intersubject variable regional anaesthesia simulator with a virtual patient architecture. *International Journal of Computer Assisted Radiology and Surgery*, 4(6):561–570, November 2009.
- [40] S. Ullrich, J. Mendoza, A. Ntoubas, R. Rossaint, and T. Kuhlen. Haptic Pulse Simulation for Virtual Palpation. In *Proceedings Bildverarbeitung für die Medizin 2008*, pages 187–191, Berlin, Germany, April 2008. Springer Verlag.
- [41] S. Ullrich, D. Rausch, and T. Kuhlen. Bimanual Haptic Simulator for Medical Training: System Architecture and Performance Measurements. In *JVRC11: Joint Virtual Reality Conference of EGVE - EuroVR*, pages 39–46, Nottingham, UK, September 2011. Eurographics Association.
- [42] R. Williams II, J. Howell, and R. Conatser Jr. *Handbook of Digital Human Modeling for Applied Ergonomics and Human Factors Engineering*, chapter Digital Human Modeling for Palpatory Medical Training with Haptic Feedback. CRC Press, 2008.
- [43] R. L. Williams II, J. N. Howell, and D. C. Eland. The virtual haptic back for palpatory training. In *International Conference on Multimodal Interface 2004*, pages 191–197, Pennsylvania, USA, October 2004.
- [44] Y. Zhang, R. Phillips, J. Ward, and S. Pisharody. A survey of simulators for palpation training. *Studies in health technology and informatics*, 142:444–446, 2009.
- [45] C. B. Zilles and J. K. Salisbury. A constraint-based god-object method for haptic display. In *Proceedings of the 1995 IEEE/RSJ International Conference on Intelligent Robots and Systems*, volume 3, pages 146–151, Pittsburgh, PA, 1995.